# Spin induced aerodynamic flow conditions on full-scale aeroplane wing and horizontal tail surfaces

**R. I. Hoff**
**rein.hoff@brunel.ac.uk**
**G. B. Gratton**
**guy.gratton@brunel.ac.uk**
Brunel Flight Safety Laboratory
School of Engineering and Design
Brunel University
Uxbridge, Middlesex, UK

## ABSTRACT

The aerodynamic flow conditions on wings and tail surfaces due to the rotational motion of a spinning aeroplane have been investigated in a full-scale spin flight research programme at the Brunel Flight Safety Laboratory. The wing upper surface vortex has been visualised using smoke and tufts on the wing of a Slingsby Firefly. The flow structures on top of both wings, and on top of the horizontal tail surfaces, have also been studied on a Saab Safir. The development of these rotational flow effects has been related to the spin motion and the effect on the spin dynamics has been studied and discussed. Evidence suggests that the turbulent wake from the wing upper surface vortex impinges the tail of the aircraft during the spin entry. It is hypothesised that the turbulent flow structure on the outside upper wing surface is due to additional accelerations induced by the rotational motion of the aeroplane. Furthermore, the lightening in stick force during spin entry and the apparent increase in push force required for spin recovery corresponds to the observed change in flow condition on the horizontal tail. The difference in pressure on the upper and lower horizontal tail surfaces have been measured using differential pressure sensors, and the result corresponds both with the observed flow conditions and earlier research results from NASA.

**Paper No. 3966.** Manuscript received 28 February 2012, revised version received 29 August 2012, second revised version received 18 September 2012, accepted 26 September 2013.

# NOMENCLATURE

| | |
|---|---|
| $\mathbf{a}$ | total flow acceleration vector |
| $\mathbf{a}_u$ | local flow acceleration vector |
| d$P$1 | differential pressure sensor No 1 |
| d$P$2 | differential pressure sensor No 2 |
| d$t$ | time step |
| $p$ | roll rate |
| $q$ | pitch rate |
| $r$ | yaw rate |
| $\mathbf{R}$ | radius vector |
| $\mathbf{v}$ | flow velocity vector |
| $\alpha$ | angle-of-attack (alpha) |
| $\Omega$ | rotation rate or angular velocity vector |

### *Abbreviations*

| | |
|---|---|
| AHRS | Attitude and Heading Reference System |
| BFSL | Brunel Flight Safety Laboratory |
| CAS | Calibrated Air Speed |
| CFD | Computational Fluid Dynamics |
| CG | Centre of gravity |
| FDR | Flight Data Recorder |
| GPS | Global Positioning System |
| IAS | Indicated Air Speed |
| IMU | Inertial Measurement Unit |
| LEV | Leading Edge Vortex |
| LSA | Light Sport Aircraft |
| MAC | Mean Aerodynamic Chord |
| MATLAB | Matrix Laboratory |
| MEMS | Micro Electro Mechanical System |
| NACA | National Advisory Committee for Aeronautics |
| NASA | National Aeronautics and Space Administration |
| PSG | Post-stall gyrations |
| RAE | Royal Aircraft Establishment |
| TDPF | Tail Damping Power Factor |
| USV | Upper Surface Vortex |

# 1.0 INTRODUCTION

Predicting an aircrafts spin characteristics, and in particular its spin recovery characteristics, before a flight test programme is very difficult. A case in point might be the problems Cessna had during certification testing of the Cessna 162 Skycatcher Light Sport Aircraft (LSA). One prototype aircraft was lost during spin testing after the test pilot had to bail out[1], and later there was another spin testing incident where another prototype aircraft was damaged[2]. Eventually, after design modifications had been implemented, the spin testing programme for the Cessna 162 was completed. Unfortunately, this case is probably not unique and there have been several cases of spin recovery problems encountered during spin flight testing resulting in loss of prototype aircraft (e.g. Lancair 400 [3], Gippsland GA-8 Airvan[4], Airplane Factory Sling[5,6]).

https://doi.org/10.1017/S0001924000008824 Published online by Cambridge University Press

Due to the lack of a reliable spin recovery prediction method, the test pilot is basically left with a careful, incremental, but nonetheless still hazardous spin testing method. A spin flight-testing programme of a light, low-wing, amateur-built aircraft in Norway, with one of the authors (Hoff) as Test Pilot, became the background for a spin research programme at Brunel Flight Safety Laboratory (BFSL). While searching for a spin recovery prediction method, being relevant due to a modified tail on the amateur-built aircraft, it became clear that several spin research questions should be addressed. In particular, the effectiveness of rudder and elevator for spin characteristics and recovery, and also the unsteady aerodynamic flow over wing and tail areas should be better understood before a spin prediction method would become a future reality.

A full-scale experimental spin research programme was thus launched using a military type trainer, the Slingsby T67M200 Firefly as the research aircraft. The first stage in this research programme was capturing the spin motion for use in later analysis and also studying the flow over wings and empennage using wool tufts. The tufts revealed a vortex forming on top of the outside wing during the spin. This Upper Surface Vortex (USV) formed and moved outwards as the spin developed and moved inwards again during the spin recovery. Furthermore, a Leading Edge Vortex (LEV) was observed on top of the outside horizontal tail. This previous work has been reported earlier at the 4th European Flight Test Safety Workshop[7] and details published in *The Aeronautical Journal*[8].

In this paper the second stage of this research is presented. Smoke has been used to visualise the flow conditions on the wing, in particular the formation and development of the USV and how the generated vortical flow is shed downstream. To check if the aerodynamic flow structure observed was unique for the research aircraft, full-scale research flights have also been flown using another military trainer type aeroplane, the Saab Safir, and the results compared. To further investigate the aerodynamic flow conditions on the horizontal tail, the difference in pressure between upper and lower surfaces has been measured using differential pressure sensors. Finally, these results are then discussed and compared to earlier wind-tunnel research results from NASA.

## 2.0 BACKGROUND

Historically, the aerodynamic forces, of particular interest due to an aeroplane spin, have been those related to the autorotation of the wings and the damping effect of the vertical tail surfaces. The classical explanation of aerodynamic forces in the spin is typically that the autorotation of the wings are driving the spin and the tail provides the damping, thereby creating a balance in aerodynamic forces for the steady spin. The autorotation of the wings is normally described (e.g. by Stinton[9]) as initiating due to one wing going up, and the other going down. The difference in angle-of-attack due to this relative motion results in autorotation due to one wing having lower angle-of-attack (more lift, less drag) and the other having higher angle-of-attack (less lift, more drag).

There are many accidents yearly due to stall/spin related loss of control. Typically, for such accidents the airspeed is inadvertently reduced below the normal range for safe flight, one or both wings reach the critical angle-of-attack, and if the impending stall is not promptly recovered, a spin might develop due to an asymmetric lift condition (i.e. autorotation). Unfortunately, the result is often fatal for the pilot and passengers, in particular when the stall/spin is entered at a height above ground where recovery is not possible before impact. Due to the continuation of stall/spin related loss of control accident rates for light aeroplanes worldwide, the problem can be described as unresolved.

NASA, and its predecessor NACA, has conducted aircraft spin research since the 1930s. Of

https://doi.org/10.1017/S0001924000008824 Published online by Cambridge University Press

particular interest, and relevant background for the current spin research at BFSL, has been NASA's Tail Damping Power Factor (TDPF), built upon earlier research at RAE in the 1930s. In a nutshell, the TDPF considers the aeroplane tail geometry and its mass distribution, and by using empirical data indicate the chances of recovering from a developed spin. One could say that the TDPF related research went through several cycles with a gradual decline in acceptability, from suggested use as a tail design criterion for safe spin recovery, to 'use with caution' due to the limited considerations from other effects (e.g. the wing) on the spin, and finally 'do not use' because the assumptions used initially were wrong.

In this final discounting of the TDPF in the NASA study from 1989[12], they measured the empennage and aft fuselage surface pressure on a 1/7-scale model in the wind tunnel ('Spin Tunnel'). While investigating aeroplane spin dynamics, isolating the aerodynamic effects from the inertia effects is a real challenge. Measuring pressures on lifting surfaces is clearly a very direct method for investigating aerodynamic force. In the wind tunnel they tried several configurations, e.g. taking alternately the wing and horizontal tail off the complete aeroplane configuration, and they concluded that both the wing and horizontal tail influence the pressure distribution on the tail in an adverse sense (reduced 'damping' of yawing moment). Furthermore, they measured negative pressure on top of the horizontal tail and suggested that this negative pressure influence the pressure on both sides of the vertical tail.

The use of wind tunnel to investigate spin dynamics is unique due to its flexibility in controlling test conditions and modifying the aeroplane model (e.g. the unlikely configurations such as wing and horizontal tail off). However, the results from spin wind tunnels should always be treated with caution due to its limitations. One limitation is the scale effects when using a small aeroplane model (e.g. the difference in Reynolds number). Another is the fact that the aeroplane spin is usually constrained, e.g. in the NASA study the spin axis was fixed through the aeroplane CG (at 25% MAC), and limited to a study of a steady state spin condition. On the other hand, in experimental full-scale spin research, controlling test conditions is difficult and modifying or instrumenting airworthy aeroplanes are challenging. However, scale effects are not an issue and the 'free' spin, including the dynamic transitions of spin entry and recovery, can be investigated. Therefore, full-scale flight research data should ideally be used to validate spin wind-tunnel results.

Another research organisation that has contributed to full-scale spin research is the Canadian National Research Council (NRC). They investigated a high-rate, low alpha ($\alpha$) spin mode using a North American Harvard[13]. The Harvard is, like the Saab Safir, a vintage military trainer type aeroplane. They studied the aerodynamic flow conditions on the wing and described the differences in flow conditions such as separated and attached flows, and also described vortices on the wing surfaces using video imagery and tufts. However, the vortices described in that study were not of the scale as seen on the Slingsby, where the diameter of the vortex was comparable to the wing chord, nor was the spanwise movement on upper wing surface as the spin developed described.

There has also been interest in full-scale high angle-of-attack research for modern fighter aircraft. Due to a tactical requirement to operate at higher angles of attack there have been specific interest in design features, such as leading edge root extension fences and thrust vectoring, which enable controlled flight at high alpha. For example, during the 1990s NASA used a modified F/A-18A fighter aircraft (the High Alpha Research Vehicle) to investigate the flow conditions during high angle-of-attack flight. They used both on-surface (e.g. dye, tufts and flow cones) and off-surface (e.g. smoke) techniques to study the flow, especially the vortices emanating from the nose section and from the leading edge root extensions were scrutinised[14].

https://doi.org/10.1017/S0001924000008824 Published online by Cambridge University Press

In addition, this aircraft was instrumented to measure the pressure distribution on both wings and these measurements were then compared with the flow visualisation results[15].

## 3.0 EXPERIMENTAL SETUP

For the Slingsby Firefly, the experimental setup included use of wool tufts, several cameras and a boom mounted to the wing to hold a smoke source. The boom was designed and built specifically for this project. The primary aim of the smoke boom was to put the smoke source on the wing where the USV could be visualised. Therefore the smoke source was put where the vortex seemed to have the greatest radius and ahead of, slightly above, the wing leading edge (Fig. 1). The smoke canister is the 'Comet'[16], made for use as smoke signal for sport parachuting. This is of the cold smoke class, and as the name suggest no heat is generated.

Again, as in the first stage of this research project[8], a helicopter with high-end camera equipment mounted on-board, was used as a chase aircraft. The video camera used in the helicopter was the Panasonic HPX3100 fixed in a special-purpose built camera rig with Kenyon stabilisation gyros. A camcorder was mounted on the left wingtip of the Slingsby and a micro camcorder was mounted on top of aft fuselage, in a position to capture the USV on the wing. To be able to study the vortex structure in higher fidelity a Casio Exilim F1 was used in the 300 frames per second mode, shooting the tufts and smoke trail on the wing from the cockpit.


Figure 1. The Slingsby Firefly research aircraft in flight. Note the smoke boom attached to the wing, wool tufts on the right wing and also on the horizontal tail surfaces.

https://doi.org/10.1017/S0001924000008824 Published online by Cambridge University Press

Cameras and tufting technique were also used on the Saab Safir aeroplane. However, smoke was not used for flow visualisation on the Safir, nor was the helicopter used for chase, but a Flight Data Recorder (FDR) was used to measure data for use in analysis. In addition, the difference in pressure between upper and lower horizontal tail surface was measured on the Safir using a modified electronic Pitot-static system.

### 3.1 The MTi-G flight data recorder

An MTi-G[17] Flight Data Recorder (FDR) was used to measure the angular velocity components; roll, pitch and yaw rates (*p, q, r*). The MTi-G is an integrated GPS and Inertial Measurement Unit (IMU) with a Navigation, Attitude and Heading Reference System (AHRS) processor. The rate of turn sensor is a Micro Electro Mechanical System (MEMS) solid-state type. The rotation rate, omega (Ω), was estimated using the following equation:

$$\Omega = \sqrt{p^2 + q^2} + r^2 \quad \ldots (1)$$

To be able to determine the start and end of the spin from the recorded data only, without recording the position of the flight controls, the following spin criteria were used (when recording data at 25Hz):

- Start of spin at time where |p| > 1, minus 35 time steps (1·4sec)
- End of spin at time where |p| < 0·1, plus 25 time steps (1sec)

These start and end of spin criteria were crosschecked and confirmed valid by studying the Euler angles, e.g. the start time correspond with pitch angle increase due to full back stick.

Furthermore, to establish the turn completions from recorded data, a technique was used where rotation rate is integrated with respect to time and then divided by the circumference:

$$\text{No. of turns} = \frac{\int \Omega \, dt}{2\pi} \quad \ldots (2)$$

This technique of integrating Ω has earlier been used in other spin flight test programmes (e.g. as reported by Muller and Pommera[18]). A MATLAB program was written for this research project, where estimated omega from Equation (1) was integrated using trapezoidal integration for every time step as the spin developed. For every consecutive natural number, the time step was saved and the number of turns shown as a vertical line together with the plotted parameter. For example, the Appendix shows the Saab Safir yaw rate for three 6-turn spins. The turn completions from the first 6-turn spin are shown as vertical lines.

A comparison was made of time elapsed in the Slingsby 2-turn left spin from 1st turn to 2nd turn. From the vision-based state estimation[8], time elapsed was 2·2secs versus 2·1secs from the integration of omega technique described above. The difference was within 5%, which is a reasonable agreement between these two methods. It should however be noted that these two spins were not flown on the same flight and a slight difference in spin characteristics could be possible from one flight to the other.

### 3.2 The PSS-8 pressure sensor system

A modified electronic Pitot-static system, the PSS-8/WT[19], was used to measure the difference in pressure between the upper and lower horizontal tail surface. The electronic circuit board (Fig. 2) has two differential pressure sensors and the pressure differential was measured on the lifting surface

https://doi.org/10.1017/S0001924000008824 Published online by Cambridge University Press

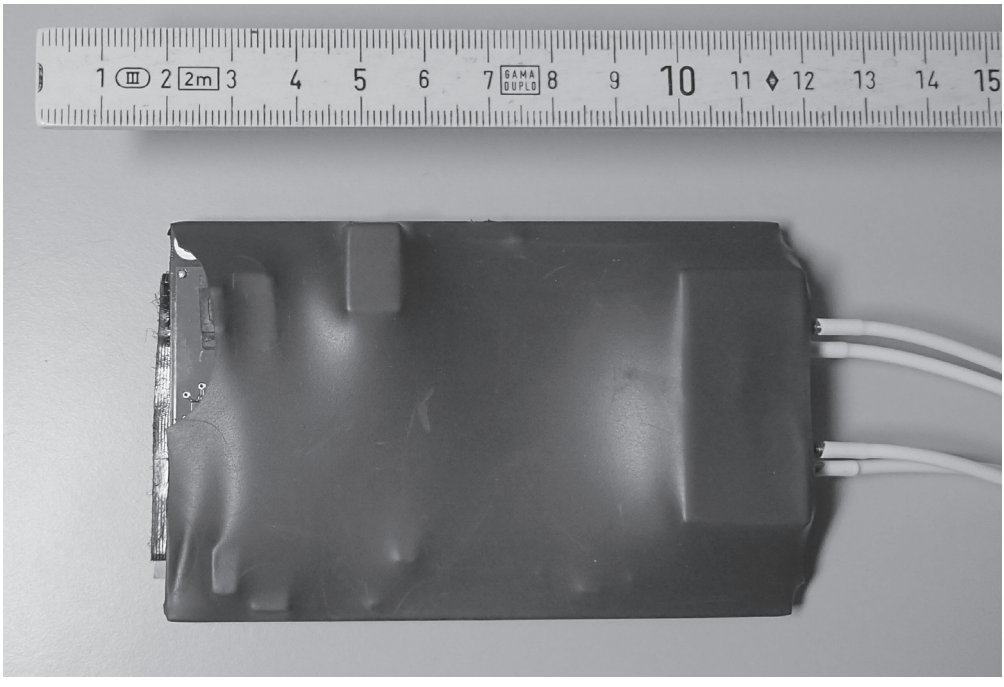

Figure 2. The modified Pitot-Static system circuit board with two differential pressure sensors. The plastic tubes are connected to the pressure ports on the right hand side of the circuit board.

using plastic tubes connected to the circuit board. The pressure ports are 2mm in diameter and one is defined as a '+' port and the other as a '–'port. The sign convention is only a definition, e.g. if pressure is higher at the '+'port the differential pressure is positive, and conversely if the pressure is higher on the '–'port the result is a negative differential.

Aerodynamically, the optimal approach for measuring static pressure on a lifting surface would be to drill holes in the surface and connect the pressure measurement tubes from the inside. However, an airworthy aeroplane was used for this full-scale research and drilling holes in the surface would clearly modify the structure and was thus not acceptable. Therefore, small (2mm internal diameter) plastic tubes were routed from the circuit board installed in the aft fuselage to the desired points on the surface as shown in Fig. 3. The risk when using this technique for surface pressure measurements is 'pollution' of data if a dynamic pressure component is measured in addition to the static pressure. For the present spin research application this scenario is possible if any net reverse flow is present on the lifting surface. While testing this pressure measurement technique on a point on the upper Safir wing, reverse flow was indeed observed in the data traces as 'spikes', e.g. the differential pressure suddenly shifting sign due to the sudden increase in dynamic pressure. Therefore, to be able to use this pressure measurement technique, a detailed knowledge of flow direction (e.g. by using tufts on the surface) is required to identify time frames where the flow direction is aligned with the tube inlets.

The pressure data were logged at 100Hz using the same computer used to obtain data from the MTi-G data recorder. Data from the two sensor platforms were synchronised post-flight. The MTi-G manual list an orientation worst case acquisition and computation time of 5·38ms for the aerospace scenario and output mode[17]. For the PSS-8/WT, a delay in the system of 10ms could

https://doi.org/10.1017/S0001924000008824 Published online by Cambridge University Press


Figure 3. The modified Pitot-Static system circuit board was installed in the aft Saab Safir fuselage and the plastic tubes were routed on upper and lower surface to the desired points used for measurement (two points on the upper surface and two points on the lower surface). Tube marked dP1 was connected to the first, and dP2 was connected to the second differential pressure sensor.

be expected if a 3m tube length was used[20]. The longest pair of tubes used for measurements was 1·38m for differential pressure sensor 1 (dP1). For the present research application these delays were considered to be well within the accuracy required.

### 3.3 Spin entry and recovery techniques

The primary aim of this research was to study the aeroplane spin in atmospheric conditions. Research flights in the atmosphere are more challenging due to the non-controlled environment, as compared to a controlled environment typical of a laboratory or wind tunnel. It was essential that the exact same spin entry and recovery procedure be used consistently. Furthermore, since the aim was to study the aeroplane spin, post-stall gyrations (PSG) should be kept to a minimum. The spin entry technique used was the low-energy type, i.e. not accelerated, where spin entry controls are applied just before (1 knot) the stall. However, when using this spin entry technique, which compares to typical entry techniques used in a flight-training environment, PSG will most likely be evident during the entry and initial phase of the spin (2-3 turns). It is possible that other spin entry techniques could be used to minimise PSG even more, but such trials are beyond the scope of the present study. The stalling speed, from level flight, engine idle, using 1 knot/second deceleration rate and cruise configuration was 58 IAS (59 CAS) for the Slingsby Firefly and 54 IAS (54 CAS) for the Saab Safir.

The detailed spin entry procedure used is described below (from Ref. 8):

‘1. A visual reference was chosen on the ground and in front of the aeroplane. This reference was used to count the number of turns.

2. The stall was entered from level flight, with engine set to idle power.

https://doi.org/10.1017/S0001924000008824 Published online by Cambridge University Press

3. Speed was reduced towards stall speed (deceleration rate 1knot/sec.). At just before (1 knot) the indicated stall speed, spin controls were set simultaneously. If spinning to the left, spin controls were full left rudder and full aft stick with ailerons centred.
4. The aeroplane entered the spin, and turns counted when passing the reference mark chosen on the ground.'

At the required number of spin turns, the spin recovery controls were set (from Ref. 8): 'For a left turn spin, the rudder was set from full left to full right (rudder reversed). After the rudder was set full opposite the turn direction, the stick was centrally moved forward until the spin stopped.'

## 4.0 UPPER SURFACE VORTEX SMOKE VISUALISATION

Due to tuft observations on the vertical tail during the 2-turn Slingsby spin[8], it was hypothesised that the wake from the USV on the wing momentarily impinged the tail surfaces. To further investigate this possible turbulent wake generating effect and discover if it indeed impacted the tail, smoke was used to visualise the flow. It was also hoped that smoke would give a better 3D view of the turbulent upper wing boundary layer.

During the left spin entry, as the elevator was moved to the full up position, the wing on-surface vortex moves outwards and the smoke is pulled inwards and towards the fuselage. The angle of the smoke trail is initially towards the tail, but did not hit the tail itself (revealed by the tail-mounted camera). The smoke trail was clearly deflected upwards at the first peak in alpha ($\alpha$), before it again followed the wing contour as the tufts indicated streamline flow over the whole wing.

From the ½-turn point, as soon as the vortex again formed on the outside wing, the smoke was pulled inwards toward the fuselage (Fig. 4). From the ½-turn to 1-turn point, tail and aft fuselage was covered in smoke (Fig. 5). From the 1-turn point, the smoke trail was aligned with (parallel to) the fuselage and did not interfere with the tail section of the aircraft. However, as the aircraft approached the 1½-turn point, smoke was visible towards the fuselage. The main smoke trail was going straight back from the wing, but a portion of the smoke was clearly deflected towards the fuselage.

From the 1½-turn point, smoke was clearly visible from the smoke source and over the entire wing towards the fuselage. Before the 2-turn point, smoke was also visible on the outer section of the wing towards the wing tip (Fig. 6). This indicates that the observed on-surface vortex moving towards the wing tip sucks some smoke outwards. After the 2-turn point, and after recovery action commenced (with full right rudder), smoke was covering the whole length of the wing.

As the elevator was moved forward for the recovery, the nose of the aircraft was pitching down and the smoke indicates transition to streamline flow. Figure 7 clearly shows the turbulent wake being left behind as the aircraft recovers and dives out of the spin.

## 5.0 SAAB SAFIR – A SPECIAL CASE OF RUDDER CONTROL LIMITING

To check if the observed phenomenon, in particular the USV on wing and LEV on top of horizontal tail, was unique to the research aeroplane used, spin flights were also flown with another military

https://doi.org/10.1017/S0001924000008824 Published online by Cambridge University Press

Figure 4. Smoke is pulled inwards by the USV as it moves towards the wing tip during the spin entry (from the ½-turn point). The top and bottom images, from the helicopter chase and the cockpit camera respectively, are synchronised.

https://doi.org/10.1017/S0001924000008824 Published online by Cambridge University Press


Figure 5. Smoke visualisation before the 1-turn point in the left spin.

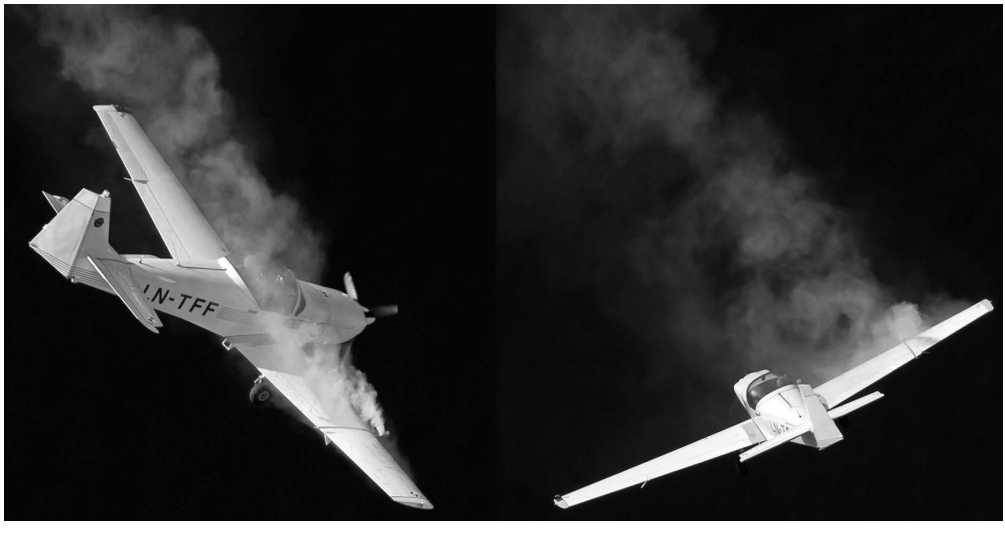


Figure 6. Before the 2-turn point (left image) in the spin, and after full right rudder was applied for the recovery at the 2-turn point (right image), smoke was visible towards the wing tip.

https://doi.org/10.1017/S0001924000008824 Published online by Cambridge University Press

Figure 7. Aeroplane recovers from the spin.

trainer type aeroplane. The Saab Safir is also a low-wing, aerobatic category, military primary trainer, but from an older generation (first model flown in 1945). The general layout of the Safir is shown in Fig. 8 opposite.

The Safir has a special rudder design feature. The rudder is twisted so that it is more effective to the right than to the left. According to the Airplane Manual[21]: 'The rudder is slightly washed out to the right side to compensate torsion impulses from the propeller slip stream'. This rudder washout can be seen in Fig. 9 next page, and due to this design feature the Safir will only spin to the right (when using the standard spin entry technique). Spins to the right, using the same standard spin entry

https://doi.org/10.1017/S0001924000008824 Published online by Cambridge University Press

and recovery technique as used previously on the Slingsby Firefly[8], were qualitatively similar to the Slingsby spin, with recovery normally after an additional ¾-turn for a 2-turn spin (after recovery controls were applied). For the 6-turn spins in the Safir, recovery was normally after additional 1¾ turn. Spin entries to the left resulted in a spiral mode. The Safir spin entry to the left, as perceived from the cockpit, was similar to the right spin entry. However, after 1 turn, the nose pitches down to a steep attitude and there was a transition to a spiral, with speed and load factor build-up. The difference in yaw rate values obtained from a total of six 2-turn spins (3 left and 3 right) can be seen in Fig. 10. One left – right spin pair was flown with another Saab Safir. However, both Safir's have the same model designation as in Fig. 8 previous page. The yaw rate in the spirals (2-turn left) was less than the 2-turn spins to the right. Eg. after 2·2 seconds, the left spins were in the range of 60 – 69 deg/sec and the right spins had 83 deg/sec. After 5·0 seconds the difference was 60 – 90 deg/sec for the left spins versus 110 – 120 deg/sec for right spins.

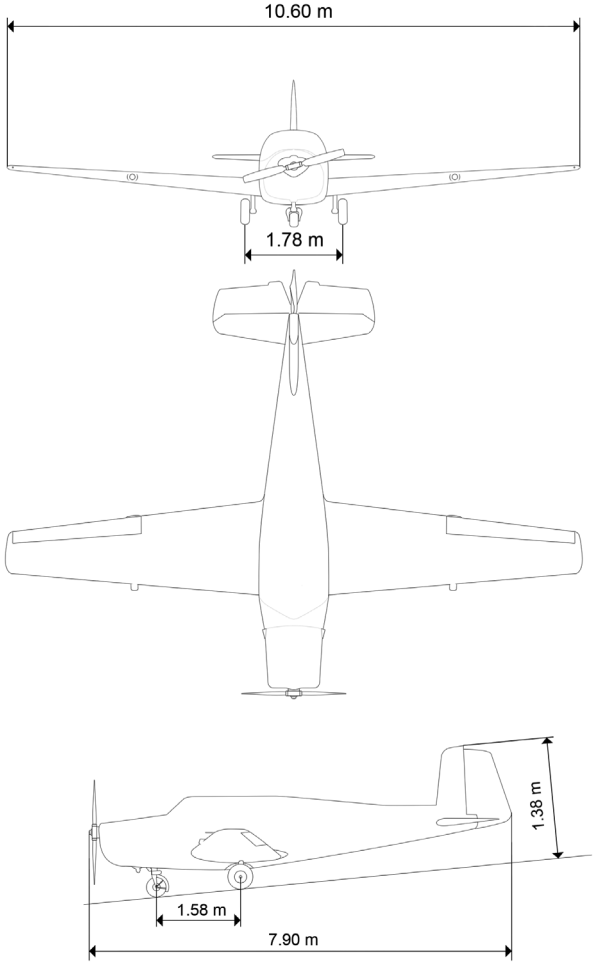


Figure 8. 3-view of the Saab Safir (model SB 91 B2) used in the BFSL spin research programme.

https://doi.org/10.1017/S0001924000008824 Published online by Cambridge University Press

Figure 9. Pictures of the Saab Safir rudder showing full left, neutral and full right positions.
Note the twisted rudder and the difference in rudder angle when displaced full left and full right.

The recovery from the spiral mode was instant with no perceived back force on the stick (as compared to a right spin in the Safir where the stick must be pushed forward for recovery). Therefore, the Safir being rudder control limited to the left but not to the right was believed to be an interesting case for studying the above mentioned flow conditions. The observed flow conditions, using tufts on the upper side of wing and horizontal tail, are described below. The outside wing was defined as the wing having relative motion forward and up in the spin (e.g. right wing in a left spin) and conversely the inside wing moving backwards and down.

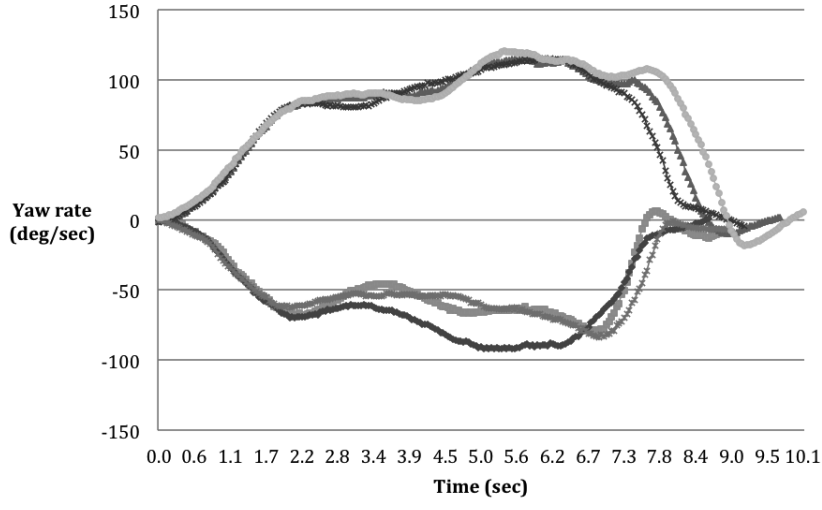


Figure 10. Measured yaw rates for Saab Safir 2-turn left (spiral mode) and 2-turn right spin. Due to right-hand sign definition, yaw to the left is negative and yaw to the right is positive. A total of 6 spins, 3 left and 3 right, were plotted and one left – right pair was measured using another Saab Safir (but of the same model).

https://doi.org/10.1017/S0001924000008824 Published online by Cambridge University Press

### 5.1 Description of observed aerodynamic flow, outside wing in a right 2-turn spin

Before spin entry, airflow separation was evident from inboard trailing edge. Flow outboard of the landing light at approx half semi-span was still streamline. At spin entry, tufts indicated unsteady flow but direction was predominantly spanwise (towards the wing tip). At ¼-turn point, a vortex centre was observed at mid-wing (just inboard of landing light position). In one of the video imagery sequences, rotational flow was clearly apparent with one tuft, second row inboard of landing light, rotating twice (720 degrees) about its centre anti-clockwise in 0·2 seconds (54 frames, 300 frames per second video imagery). In another video sequence, the same tuft was also observed to rotate, but only once (360 degrees) in 27 frames (0·1 sec), half the time of the previously mentioned double rotation. This tuft rotation rate is about 30 times the rotation rate

Figure 11. Illustration based on the flow direction indicated by tufts, showing the dipolar vortex structure temporarily observed on the outside wing of the spinning Safir after the 1-turn point in the right spin.

https://doi.org/10.1017/S0001924000008824 Published online by Cambridge University Press

of the aeroplane, which is at least an order of magnitude difference.

Towards the ½-turn point, the outer part of wing from 2 rows of tufts inboard of landing light were streamline. After the ½-turn point the vortex moved outwards again and at ¾-turn flow were streamline from 2 rows of tufts outboard of landing light, with the flow predominantly spanwise behind. Spanwise flow was still predominant at 1-turn point with tufts deflecting aft (streamline) at the wing-tip area. However, from the 1-turn point, a dipolar vortex structure was observed, with anti-clockwise rotational flow outboard of landing light and 3-4 rows of tufts inboard of landing light were indicating reverse flow. The tufts furthest inboard (nearest the fuselage) were temporarily deflected in the clockwise direction. An illustration of this flow structure can be seen in Fig. 11. However, although this flow structure was observed in the video imagery over several frames (about 50 – 60 frames which is 0·16 – 0·2 seconds) the flow was very unsteady with every single tuft deflecting slightly from frame to frame, sometimes against the 'perfect' circular flow direction.

Vortex rolls back from 1¼ turns and the tufts outboard of landing light were streamline again. However, from 1½-turn point vortex rolls out again and the aforementioned dipolar structure are again evident at 2-turn point. Spin recovery actions were started from 2-turn, and the vortex started to move back from 2½-turn and recovery was complete at 2¾-turn where rotation ceased and flow became streamline over wing. A summary of observations as described in this section is shown in Table 1.

**Table 1**
**Summary of tuft observations on outside wing from the Safir 2-turn right spin**

| Time (sec) | Spin position | Tuft observations |
|---|---|---|
| 0 | 0 | Airflow separation from inboard trailing edge. Predominantly spanwise flow (outwards) from spin entry. |
| 1 | ¼ | Vortex centre at mid-wing (just outboard of landing light). |
| 2 | ½ | Outer part of wing had streamline flow. |
| 3 | ¾ | Vortex moved outwards, with flow predominantly spanwise behind. Outer part of wing was still streamline. |
| 4 | 1 | Spanwise flow predominant over wing, except the wing-tip area, which had streamline flow. |
| 4+ | 1¼ | Dipolar vortex structure, anti-clockwise rotational flow outboard, reverse flow in-between and clockwise rotational flow inboard. |
| 5 | 1½ | Outer part of wing had streamline flow again. |
| 6 | 2 | Dipolar vortex structure as described above was again evident. |
| 7 | 2½ | Vortex moved towards fuselage, flow over wing becoming streamline. |
| 8 | 2¾ | Spin recovery (rotation ceased) and flow streamline over full wing. |

## 5.2 Description of observed aerodynamic flow, inside wing in a left 2-turn spin (spiral mode)

Spin entry to the left was initially similar to the right spin entry, with separation starting at inboard trailing edge and flow deflecting outboard as the stall progresses. However, with the

https://doi.org/10.1017/S0001924000008824 Published online by Cambridge University Press

relative back- and downward motion of the left wing in a left spin, the flow quickly separates on the whole wing surface. The flow was unsteady and irregular, with some of the tufts along the leading edge temporarily going straight up, normal to the wing surface. At ¼-turn the flow is still irregular, but reverse flow on most of the wing surface is predominant. Compared to the outside wing flow, the row of tufts on the wing tip on inside wing, was indicating either reverse or spanwise flow. Also, it was difficult to observe any clear pattern, e.g. with one tuft in streamline direction and the next in reverse direction (erratic motion). From ¼-turn, this flow condition continued until spin recovery, but with some time frames where reverse flow was more apparent. At recovery, flow reattachment started from the wing tip and after 48 frames (1/6sec) the whole wing was streamline again.

## 5.3 Description of observed aerodynamic flow, outside wing in a left 2-turn spin (spiral mode)

At entry flow separated from inboard trailing edge and flow was deflected outboard, indicating spanwise flow. However, flow outboard of landing light remained streamline, and after ¼-turn towards the ½-turn point, more flow became streamline and only an area inboard towards the trailing edge was separated. After ½-turn point the tufts again indicated spanwise (outward) flow, but flow outboard of landing light was still streamlined and remained so for the rest of the spin. From the 1-turn point, again only an area inboard, aft at the trailing edge was separated and the row of tufts along the leading edge was all streamline. All the tufts indicated streamline flow from the 1½-turn point to the (instant) recovery at 2-turns.

## 5.4 Description of observed flow on the horizontal tail surfaces

Due to limitations on the small tail camera used (only 20 frames per second), it was not possible to study the flow in the same fidelity as on the wing where a camera capable of 300 frames per second was used. However, it was still possible to see some notable differences, depending on spin direction, in flow conditions on the horizontal tail.

### *Left 2 turn spin (spiral mode)*

**Right horizontal tail**: As the elevator was moved to the full up position (stick full back position) and the aeroplane started to rotate left, the tufts on top of the horizontal tail surface indicated flow separation (erratic motion). At the ¼-turn point, the tufts indicated unsteady, but streamline flow. Temporarily, the tufts indicate unsteady flow, but clearly the flow was predominantly in the streamline direction during the rest of the spin.

**Left horizontal tail**: At spin entry flow separated, tufts indicated mostly erratic flow, however some frames showed spanwise (outwards) and some frames indicated unsteady streamline flow. Two frames before elevator moved down, the tufts indicated unsteady streamline flow. As the elevator reached the neutral position, the tufts indicated streamline flow (Fig. 12).

### *Right 2-turn spin*

**Right horizontal tail**: Flow separated at entry, indicating erratic flow motion. However, from just before 1-turn point, the tufts on the leading edge indicated spanwise flow (toward the fuselage). This continued for another 9 frames (20 frames per second). The flow was clearly unsteady, but a predominant direction was towards the fuselage. At 2-turn point the tufts indicate erratic flow. As the elevator started moving down (for the spin recovery), separated flow was still indicated for the next 6 frames, before it became streamline.

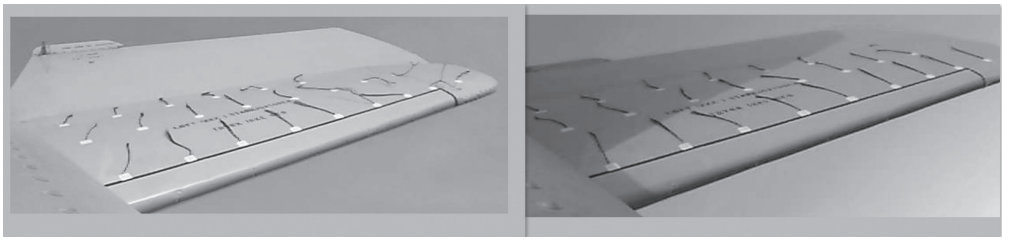

Figure 12. Tufts indicating unsteady streamline flow on left horizontal tail surface in a left, 2-turn spin, just before the elevator moves down for the recovery to the left, and elevator in neutral position on the right.

Figure 13. Tufts indicating spanwise flow on the left horizontal tail surface in a right hand 2-turn spin (at approx. the ¾-turn position in the spin).

**Left horizontal tail**: Flow separated at entry and was erratic up to the ¾-turn point, where tufts indicated flow in a predominantly spanwise outward direction (Fig. 13). Like for the inside tail surface in a 2-turn right spin, the tufts indicated flow mostly in the spanwise direction, although some frames showed erratic flow motion. Again, as the elevator started to move down for the spin recovery, the flow remained separated for 6 more frames. The elevator had moved to its neutral position after 4 frames.

## 5.5 Measurement of differential pressure between upper and lower horizontal tail surface

The difference in pressure was measured at two points on the horizontal tail surface of the Safir as shown in Fig. 3. In pre-stall flight, the horizontal tail surface exerts a down force. This was confirmed in the measurements, as the pressure was relatively lower on underside, which means relatively higher pressure on the upper surface. The speed was varied during two cycles of forward and aft stick (elevator moved forward then down) and the pressure difference changed with varying speed. Then the speed was decayed towards stall, and the pressure difference went correspondingly towards zero.

Thereafter, a series of spins were flown and the pressure difference measured. Above in Figs 14 and 15 are the results from a 6-turn right spin. The points are designated dP1 and dP2, where dP2 is the point nearest the aft fuselage and dP1 is the point furthest out on the horizontal stabiliser

https://doi.org/10.1017/S0001924000008824 Published online by Cambridge University Press

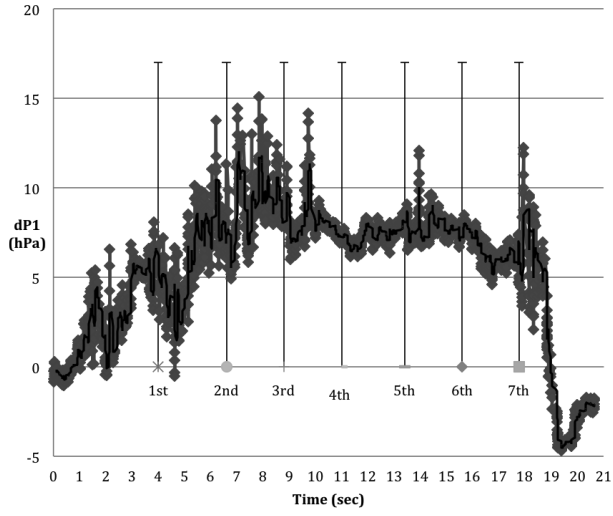


Figure 14. Difference in pressure measured at point dP1 during a 6-turn right spin in the Safir (Saab model SB 91 B2 with serial number 344, CG at 11% MAC, weight was 979kg and spin entry was at approx. 4,800ft density altitude). A 10-point moving average trend is shown as a black solid line.

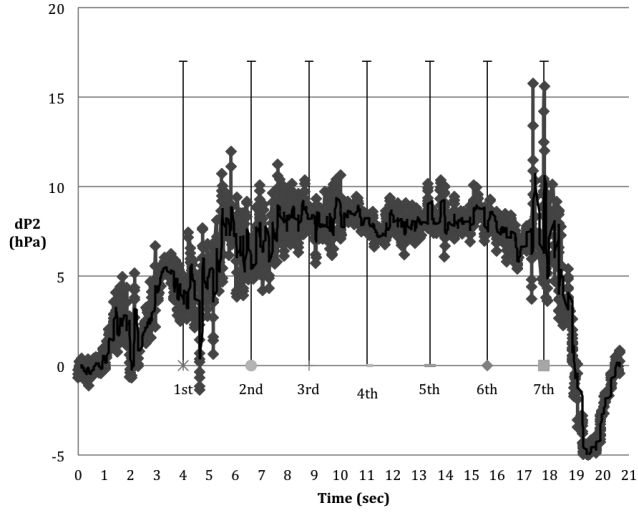


Figure 15. Difference in pressure measured at point dP2 during a 6-turn right spin in the Safir (exactly same spin as above for the dP1 measurement). A 10-point moving average trend is shown as a black solid line.

(see Fig. 3). The '–' port of the differential pressure sensor was placed at the upper surface. The results shown in Figs 14 and 15 below shows a positive pressure delta, which means a relatively higher pressure on the lower side of the horizontal stabilisator. Therefore the relatively lower pressure on the upper side exerts an up force at the tail. Note the increase in pressure difference at the ¾-turn point in the spin and a further increase at the 1½-turn point in the spin. Thereafter, the pressure delta stabilises at approximately 8 hPa from the 2-turn point. At recovery, the pressure difference changes sign back to negative as it was for the pre-stall flight regime which was lower pressure on the underside, exerting a down force at the tail.

https://doi.org/10.1017/S0001924000008824 Published online by Cambridge University Press

# 6.0 DISCUSSION

## 6.1 Rotational aerodynamic flow effects

The rotational aerodynamic flow effects appear to be due to the aeroplanes' rotation in the spin. One such rotational effect is the autorotation of the wings due to the difference in motion of up- and down-going wing. This difference in lift generation have been qualitatively observed in the present investigation, e.g. the streamline flow over the outer part of the outside wing compared to the separated, irregular flow on the inside wing. Further remarks on the autorotation of wings will be given below, but first we will discuss other observed rotational effects.

Although the USV observed on the Saab Safir outside wing did not have the same perfect circular shape as seen on the Slingsby (e.g. the vortex visualised by smoke and tufts in Fig. 4), and although the flow condition was very unsteady, vortical flow was observed. Furthermore, the same anti-clockwise rotation of a single tuft was observed in three different video sequences of the same type of spin (2-turn right), at the same position in the spin. This indicates periodic and structured flow motion as opposed to random flow circulation or vortices. The fact that the rotation is against the spin direction, and given that the shape shown in Fig. 9, resembles a source – sink pair with a saddle point in-between, lead to the suggestion that the turbulent layer flow structure is due to the rotation of the aeroplane. This structure is similar to what can be observed in the earth atmosphere, in the form of a high-pressure, low-pressure system pair (or anticyclone – cyclone pair called a Rex block in meteorology[22]) having its characteristic shape due to the rotation of the earth.

The aeroplane in a spin must be considered as a rotating frame of reference. A fluid particle in motion in this frame of reference (e.g. moving on top of the outside wing) will have additional accelerations due to the aeroplane rotation. These additional acceleration terms are the centrifugal, Coriolis and Euler accelerations.

Initially, at spin entry as the flow starts to separate from the inboard trailing edge and flow outboard was still streamline, the pressure is lower on the outside part of the wing than the inside. Therefore, the tufts indicate spanwise outward flow as the air particles moves from relatively higher pressure to lower pressure at the outer section (towards the wing tip). As the aeroplane starts to rotate in the spin, this layer of separated flow close to the wing surface is then subject to additional acceleration terms. The total flow acceleration vector is given by (e.g. see discussion on motion relative to rotating axes in Ref. 23, or alternatively the research on the flight of the fly by Letnik and Dickinson[24]):

$$\mathrm{a} = \mathrm{a}_u - 2\Omega \times \mathrm{v} - \Omega \times (\Omega \times \mathrm{R}) - \frac{\mathrm{d}\Omega}{\mathrm{d}t} \times \mathrm{R} \qquad \ldots (3)$$

where $\boldsymbol{a_u}$ is the local flow acceleration vector (e.g. due to difference in pressure on the wing upper surface), $\Omega$ is the angular velocity vector, **v** is flow velocity vector and **R** the radius vector. The minus sign in front of these vector cross products are due to the direction definition in the co-ordinate system. Coriolis acceleration varies with rotation rate and flow velocity, centrifugal acceleration varies with rotation rate squared and radius and Euler acceleration varies with the time derivative of rotation rate and radius.

As earlier described, this flow structure was observed on the outside wing. The inside wing has different initial conditions during spin entry. As the inside wing rotates aft and downwards, the flow on the whole wing separates at the same time, and this difference in pressure due to streamline flow on the outer part of the outside wing, do not exist on the inside wing.

https://doi.org/10.1017/S0001924000008824 Published online by Cambridge University Press

Applying the right-hand rule, and using Equation (3), the Coriolis force is deflecting flow against the spin direction, the centrifugal force has direction spanwise outboard and Euler force is deflecting flow in either the streamline or reverse direction, depending on the angular acceleration vector direction. Therefore, there is correlation between the theoretical flow influences due to Equation (3) and the observations, and the following hypothesis is put forward: The turbulent layer on the upper surface, on the outside wing of a spinning aeroplane, is accelerated due to additional, spin induced accelerations.

### 6.2 Autorotation of the wings

The outside wing motion is characterised by persistent up-stroke (*X*-axis rotation due to roll), rotation about the *Z*-axis (due to positive and negative sideslip), rotation about the spin axis and periodic rotation about the *Y*-axis (due to oscillation in pitch). Conversely, the inside wing motion is characterised by persistent down-stroke and relative backward motion about the spin axis. However, it will naturally have the same rotation about the *Z*-axis and the same periodic rotation about the *Y*-axis as the outside wing. Due to this complex wing motion, combined with high Reynolds number, the autorotation of the wings is very difficult, if not impossible using current technology, to model accurately with CFD. Therefore, the exact aerodynamic force contribution, or more specifically the detailed lift distribution due to autorotation of the wings remains difficult to quantify.

The USV spanwise movement in- and outwards on the outside wing appears to be governed by the periodic rotation of the wing about the *Y*-axis. The USV moves outwards when alpha increases and moves inwards when alpha decreases. It is possible that lift enhancing streamline flow on the outer part of the outside wing, and the relative higher drag of the inside wing due to reversed and irregular flow, defines autorotation of the wings for the light aeroplane. It is also possible that a certain additional lift is due to the spanwise flow observed on the outside wing. This spanwise flow might be accelerated due to the rotational aerodynamic flow effects described above.

### 6.3 The change in flow condition over the horizontal tail

In the Safir spin, a sudden change in flow condition was observed at the ¾-turn. The flow was mainly in the spanwise direction over the outside horizontal tail (Fig. 13). A similar flow structure was earlier observed on the Slingsby Firefly, and it was then suggested that this might be a leading edge vortex[8], similar to what have been found on delta wings. However, not having been able to use smoke to visualise the flow structure over the tail, the exact structure of this flow is unknown. Using the same approach as above for the wing regarding the rotational flow effects due to the aeroplane rotation, it is likely that the spanwise flow over the horizontal tail is partly due to the additional centrifugal acceleration.

It is interesting to note a change in the spin motion of the aeroplane, which might be related to this sudden change in flow condition over the horizontal tail. On both the Slingsby Firefly and the Saab Safir, it has been observed that the aeroplane has its flattest attitude at the 1-turn point. After 1-turn, the nose pitches down and the aeroplanes spun at a steeper nose down attitude. At this stage in the spin entry, rolling, yawing and pitching rotary moments are in effect[9]. So, a pitch rate ($q$) imposed on the yawing momentum precesses and result in an increased roll rate ($p$), which again result in an increased yaw rate ($r$). Yaw and roll rate histories from a Slingsby Firefly 2-turn spin (Fig. 16) show an increase in both yaw and roll rate after the 1-turn point in the spin.

Another observation of interest regarding the difference in flow condition on the horizontal tail during the spin was the difference in stick force during recovery. Recovering from a spiral (Safir,

https://doi.org/10.1017/S0001924000008824 Published online by Cambridge University Press

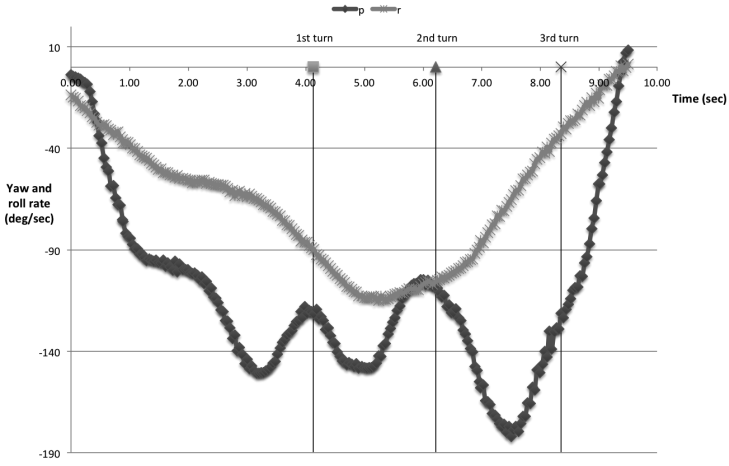


Figure 16. Yaw and roll rate time histories from a Slingsby Firefly 2-turn left spin. Note the increase in both roll and yaw rate after the 1-turn point in the spin.

2-turn left), where the flow was mostly streamline over the horizontal tail surfaces before recovery (as can be seen in Fig. 12 above), the stick moved forward as soon as stick backpressure was released. On the other hand, recovering from the spin (Saab Safir, 2-turn right), where the flow separated and spanwise flow was observed over the tail surface (Fig. 13), significant stick force (measured approx. 6kg using a hand-held scale) was needed to push the stick forward for recovery. Also, the stick force was not perceived as linear during the recovery, with the stick 'shaking' in the hand.

The data from the measurement of pressure difference between the lower and upper surface of the horizontal tail (Figs 14 and 15) indicates a reversal of horizontal stabilisator effect in the spin. The relative negative pressure measured on the upper surface is a reversal of horizontal stabilisator effect during the spin, from exerting a net nose up (down-force at the tail) to a nose down moment (up-force at the tail). From the pilots viewpoint the aeroplane is pitching nose down despite full back-stick input, which normally commands a nose-up movement, but as described above the nose of the aeroplane pitches down after the first turn in the spin. Furthermore, the delta pressure measurement corresponds with the visual observation of the sudden change in flow condition, with delta pressure value increasing from the ¾-turn point in the spin. It is also possible that the push force required on the stick for spin recovery is due to negative pressure on the upper side of the horizontal stabilisator and elevator surface. Finally, these results correspond with the NASA wind-tunnel spin research results[12], where they measured negative pressures on several points on the upper tail surfaces as shown in Fig. 17.

## 7.0 CONCLUSIONS

The former hypothesis (from the first stage of the research) was that the upper surface vortex was partly the source of turbulent flow over the empennage. Smoke, used for flow visualisation, revealed wing flow interference over the empennage during the spin entry. Apparently, even at high alpha, the smoke was pulled inwards on the wing and over the empennage before the 1-turn point. From the single smoke source, smoke was distributed over the whole wing surface, reinforcing the results from tuft observations, e.g. the existence of USV and spanwise flow.

https://doi.org/10.1017/S0001924000008824 Published online by Cambridge University Press

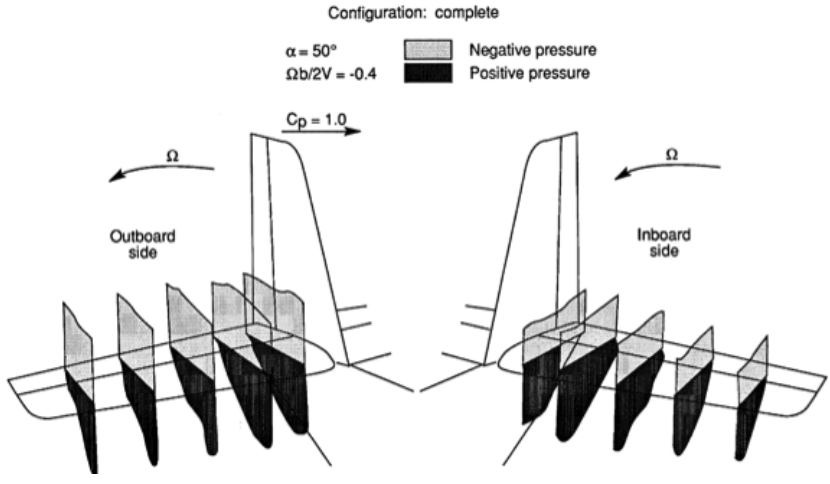


Figure 17. Measurement of pressures on horizontal tail surfaces from NASA wind-tunnel spin research. Illustration is from NASA[12].

Whilst studying the flow structure on another aeroplane type, the Saab Safir, it was found that the flow structure on the outside wing was periodic as opposed to irregular and random vortices. Although the flow in the turbulent boundary layer was very unsteady, a repeatable structure was found when examining several spins. Therefore it was suggested that the turbulent layer on the upper surface, on the outside wing of a spinning aeroplane, is accelerated due to additional, spin induced accelerations. These additional accelerations are the Coriolis, centrifugal and Euler accelerations.

A sudden change in flow condition over the horizontal tail surfaces on both the Firefly and the Safir was observed at the ¾-turn. It is suggested that this spanwise flow condition is partly due to the aerodynamic flow effects induced by the aeroplane rotation. The increase in nose down pitching moment might be related to this change in flow condition. Furthermore, the sudden stick force lightening and the subsequent increase in stick force required to push the stick forward for recovery was only found on the spin modes where this sudden change in flow condition was found. In the spiral mode, where the flow condition on the horizontal tail was predominantly streamline, the stick force lightening was not present.

Difference in pressure between the upper and lower horizontal tail surface correspond well with the visual observations of flow conditions and also correspond well with earlier pressure measurements performed by NASA in the spin wind tunnel.

## ACKNOWLEDGEMENTS

The authors are grateful to Jonny Engelsvoll for camera operation and movie production, Photographer Arne Andersen and Helicopter Pilot Kristian Elvestad for their help in providing chase for the spinning Slingsby. The authors also wish to thank Håvard Finnesand for cockpit camera operation and help with illustrations and video imagery.

## REFERENCES

1 SOBIE, B.PICTURE: Flight gets first look at redesigned SkyCatcher, Flightglobal.com, Business & GA Article, 03/02/09.

https://doi.org/10.1017/S0001924000008824 Published online by Cambridge University Press

2. TRIMBLE, S. SkyCatcher future in doubt after second flight test crash, Flightglobal.com, News Article, 20/03/09.
3. FOX, L.A. Lancair 400 Spin Testing and Spin Chute Release Failure, Proceedings of the 48th Annual SETP Symposium, 2004.
4. ROBERTS, S.C. Flight Test Lessons Learned from the Spinning Trials of the Gippsland GA-8 Single Engine General Aviation Aircraft, Proceedings of the 44th Annual SETP Symposium, 2000.
5. Sling LSA Prototype Lost During Spin Testing, EAA News, 25 February 2010.
6. South African Civil Aviation Authority, Aircraft Accident Report and Executive Summary, Sling, ZU-TAF, Ref. CA/18/2/3/8756.
7. HOFF, R.I. The Challenges of Light Aeroplane Spin Testing & Research, 4th European Flight Test Safety Workshop, London, UK, 28 September 2010.
8. HOFF, R.I. and GRATTON, G.B. Camera tracking and qualitative airflow assessment of a 2-turn erect spin, *Aeronaut J*, May 2012, **116**, (1179).
9. STINTON, D. Flying qualities and flight testing of the airplane, AIAA, Reston, VA, USA, ISBN 1-56347-274-0, 1996.
10. BOWMAN, J.S. JR Summary of spin technology as related to light General-Aviation Airplanes, NASA TN D-6575, Washington DC, USA, December 1971.
11. BURK, JR S.M. and BOWMAN, JR J.S. and WHITE, W.L. Spin-tunnel investigation of the spinning characteristics of typical Single-Engine General Aviation Airplane Designs. I – Low-wing model A: Effects of tail configurations, NASA Technical Paper 1009, September 1977.
12. BOWMAN, JR J.S., HULTBERG, R.S. and MARTIN, C.A. Measurements of Pressures on the Tail and Aft Fuselage of an Airplane Model During Rotary Motions at Spin Attitudes, NASA Technical Paper 2939, 1989.
13. BROWN, A.P. DILLON, J. CRAIG, G. and ERDOS, R. Flight Manoeuvre and Spin Characteristics of the Harvard Mk 4: Application to Human Factors Flight Research, AIAA Atmospheric Flight Mechanics Conference and Exhibit, Providence, Rhode Island, USA, 16-19 August 2004, 2004-4815.
14. FISHER DEL, D.F., FRATE, J.H. and RICHWINE, D.M. In-Flight Flow Visualization Characteristics of the NASA F-18 High Alpha Research Vehicle at High Angles of Attack, NASA TM-4193, May 1990.
15. DAVIS, M.C. and SALTZMAN, J.A. In-Flight Wing Pressure Distributions for the NASA F/A-18A High Alpha Research Vehicle, NASA TP-2000-209018, March 2000.
16. Comet, Smoke Signals for Parachutists, Data Sheet, Issue 24 April 2003.
17. MTi-G User Manual and Technical Documentation, Xsens Technologies B.V., Document MT0137P, Revsion H, 15 October 2010.
18. MULLER, D. and POMMERA, G.Spinning the modified ROBIN R2160, Cockpit, *The Society of Experimental Test Pilots*, April/May/June 1999.
19. Pitot-Static System PSS-8, Interface Definition Document, Simtec Buergel AG, Issue 1, 28 August 2012
20. Private correspondance with Simtec Buergel AG, 21 November 2012.
21. Airplane Manual SAAB SAFIR 91B-2, Description, *Control Surfaces*, 3-4.
22. `PETTERSEN, S. *Weather Analysis and Forecasting, Second Edition,* **1**, Motion and Motion Systems, McGraw-Hill, 1956.
23. MERIAM, J.L. and KRAIGE, L.G. Engineering Mechanics, *Dynamics*, 1993, **2**, 3rd ed, ISBN 0-471-59273-0.
24. LETNIK, D. and Dickinson, M.H. Biofluiddynamic scaling of flapping, spinning, and translating fins and wings, *J Experimental Biology*, 5 February, 2009, (212), pp 2691-2704.

# APPENDIX

Saab Safir yaw rate for three 6-turn spins. The turn completions from spin 'No. 1' are shown as vertical lines (which are numbered 1st, 2nd etc.).

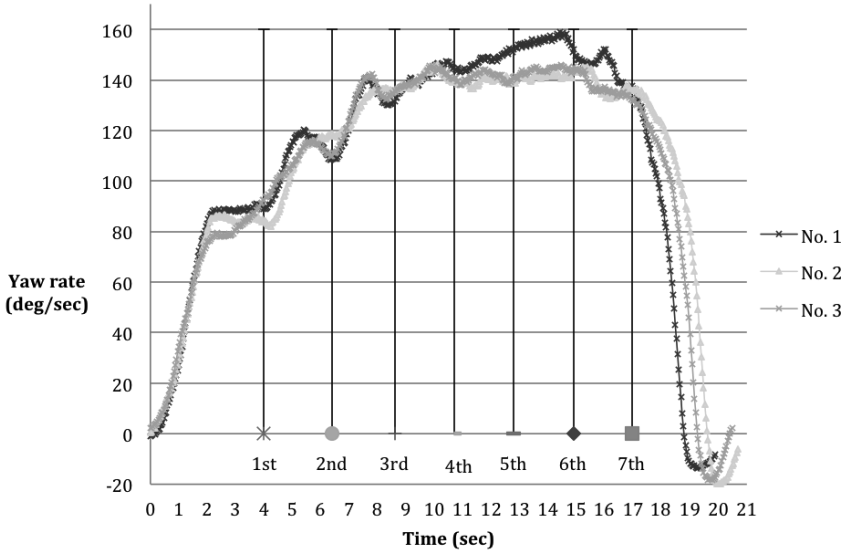


https://doi.org/10.1017/S0001924000008824 Published online by Cambridge University Press